Gas sensing properties of zinc stannate (Zn_2SnO_4) nanowires prepared by carbon assisted thermal evaporation process

T. Tharsika [a], A.S.M.A. Haseeb [a,*], S.A. Akbar [b], M.F.M. Sabri [a], Y.H. Wong [a]

[a] Department of Mechanical Engineering, Faculty of Engineering, University of Malaya, 50603 Kuala Lumpur, Malaysia
[b] Center for Industrial Sensors and Measurements (CISM), Department of Materials Science and Engineering, Ohio State University, 2041 College Road, Columbus, OH 43210, USA

ARTICLE INFO

Article history:
Received 23 June 2014
Received in revised form 18 August 2014
Accepted 22 August 2014
Available online 2 September 2014

Keywords:
Zinc stannate
Nanowires
Carbon assisted thermal evaporation
Gas sensors
Ethanol

ABSTRACT

Zn_2SnO_4 nanowires are successfully synthesized by a carbon assisted thermal evaporation process with the help of a gold catalyst under ambient pressure. The as-synthesized nanowires are characterized by X-ray diffraction (XRD), field-emission scanning electron microscopy (FESEM), and transmission electron microscopy (TEM) equipped with an energy dispersive X-ray spectroscopy (EDS). The XRD patterns and elemental mapping via TEM–EDS clearly indicate that the nanowires are Zn_2SnO_4 with face centered spinel structure. HRTEM image confirms that Zn_2SnO_4 nanowires are single crystalline with an interplanar spacing of 0.26 nm, which is ascribed to the d-spacing of (3 1 1) planes of Zn_2SnO_4. The optimum processing condition and a possible formation mechanism of these Zn_2SnO_4 nanowires are discussed. Additionally, sensor performance of Zn_2SnO_4 nanowires based sensor is studied for various test gases such as ethanol, methane and hydrogen. The results reveal that Zn_2SnO_4 nanowires exhibit excellent sensitivity and selectivity toward ethanol with quick response and recovery times. The response of the Zn_2SnO_4 nanowires based sensors to 50 ppm ethanol at an optimum operating temperature of 500 °C is about 21.6 with response and recovery times of about 116 s and 182 s, respectively.

1. Introduction

Metal oxide nanostructures with well-defined morphologies have attracted a great deal of attention because of their shape, size and surface dependent properties [1,2]. The ability to control the size and shape of nanostructures is crucial as it affects their overall properties. One dimensional nanostructures, for example, are of immense interest in the field of nanotechnology. To date, intensive studies have been carried out on binary metal oxides nanostructures in several applications [3,4]. There is a continuing need for specially designed semiconductors that has led to an interest in ternary oxides, such as Zn_2TiO_4 [5], $CdSnO_3$ [6], $ZnSnO_3$ [7], $LiNbO_3$ [8], Cd_2SnO_4 [9], Zn_2SnO_4 [10–12], $BaTiO_3$ [13], $CdIn_2O_4$ [14], $CuFeO_2$ [15], $SrTiO_3$ [13], and Cd_2GeO_4 [16]. Ternary oxides provide greater flexibility to tune the chemical and physical properties of the materials by varying the compositions [17].

Among these ternary oxides, Zn_2SnO_4 is an important n-type semiconductor with a large band gap of 3.6 eV [18], which is often called zinc tin oxide (ZTO). Studies verified that bulk Zn_2SnO_4 has high electron mobility and conductivity, good thermal stability, chemical sensitivity, and low visible light absorption [19]. For instance, Zn_2SnO_4 nanowires have been successfully used as electrodes in lithium ion batteries for its stability [20]. Hierarchical macroporous Zn_2SnO_4 nanoparticles also have highly efficient performance in dye-sensitized solar cells due to its superior light scattering ability [21]. Zigzag Zn_2SnO_4 nanowires have also been shown to exhibit high sensor performance in detecting toxic and volatile organic compounds with sensitivity towards 50 ppm ethanol around 12 [17]. Chen et al. [22] reported flower-like hierarchical Zn_2SnO_4 nanostructures based sensors that exhibited enhanced ethanol sensitivity of 8 when exposed at 20 ppm, which is ascribed to high specific surface area and increased number of surface defects. Further, hollow Zn_2SnO_4 microcrystals showed high sensitivity towards H_2S due to large surface area [23]. Recently, Park et al. [24] demonstrated that Zn_2SnO_4-core/ZnO-shell nanorod based sensors showed enhanced response to NO_2 with a sensitivity of 173–498% at a concentration range of 1–5 ppm. This value was 2–5 folds higher than that of the pristine Zn_2SnO_4 nanorod sensor owing to encapsulation of Zn_2SnO_4-core by ZnO-shell, and formation of heterojunction which acted as a lever in electron transfer. However, along with high sensitivity, there is a need to design a selective of sensor.

* Corresponding author. Tel.: +60 3 7967 4492; fax: +60 3 7967 5317.
E-mail addresses: tharsika@siswa.um.edu.my (T. Tharsika), haseeb@um.edu.my (A.S.M.A. Haseeb), akbar.1@osu.edu (S.A. Akbar), faizul@um.edu.my (M.F.M. Sabri), yhwong@um.edu.my (Y.H. Wong).

http://dx.doi.org/10.1016/j.jallcom.2014.08.192
0925-8388/

Several efforts have been made to synthesize Zn_2SnO_4 nanostructures using various processing routes such as thermal evaporation [19,25–27], hydrothermal method [28,29], catalyst-free vapour-solid process [17], solvothermal method [10,12,30], carbothermal reduction [20], and chemical vapour deposition [31]. Among these approaches, the carbon assisted thermal evaporation process is a simple and convenient way to grow large amount of Zn_2SnO_4 nanowires under ambient pressure. In the synthesis process, ZnO and SnO_2 metal oxides are simultaneously evaporated with the help of activated carbon powder. The activated carbon enhances the reaction rate by performing as reducing agent and creates the Zn and Sn vapours in an ambient pressure [32]. Then the vapours are transferred to the substrate which is at a lower temperature than the vapour source located at the center of the furnace, and reacts on the Au catalyst. Zn_2SnO_4 ternary oxide nanowires are formed based on the vapour–liquid–solid (VLS) growth mechanism [33,34]. Structural properties and optimum condition for the growth of Zn_2SnO_4 nanowires are studied by varying growth time, deposition position of the substrate and furnace temperature. Zn_2SnO_4 nanowires based sensors are configured as high performance resistor-type sensors and are used to investigate the performance of several test gases including ethanol, hydrogen and methane. Specifically, selective ethanol sensors are designed that show promising potential.

2. Experimental procedure

2.1. Synthesis of Zn_2SnO_4 nanowires

Zn_2SnO_4 nanowires were synthesized via carbon assisted thermal evaporation process under ambient pressure [35]. A schematic of the experimental setup is shown in Fig. 1(a). Commercial ZnO, SnO_2 and activated carbon powders were used as source materials. Gold interdigitated alumina was used as the substrate and 99.99% purified Ar was used as a carrier gas to transfer Zn and Sn vapour from the source to the substrate. A mixture of ZnO, SnO_2, and activated carbon powder with the molar ratio of 9:1:10 was prepared. Prior to loading the mixture inside the furnace, the powder mixture was placed in a 4.5 cm diameter jar with zirconia balls to perform planetary ball milling (Retsch PM 400). The milling was carried out for 8 h to get a homogeneous mixture of particles with an average size of 150 nm. A thin gold layer of around 40 Å thickness was applied to an alumina substrate by sputtering from a gold target at a rate of about 1.25 Å/s for 30 s using SPI module sputter coater. This Au layer is used as a catalyst to grow the Zn_2SnO_4 nanowires.

The milled powder mixture was transferred into a quartz boat and then it was placed in the center of a horizontal tube furnace (Lindberg Blue M). Then the alumina substrate was placed in various position from 3 cm to 12 cm away from the source powder at a step of 3 cm. Prior to exposure to Ar gas with a constant flow rate, the furnace was purged for 15 min to remove unwanted contamination inside the quartz tube. Then Ar was introduced with a constant flow rate of 25 sccm throughout the process. Subsequently, the temperature of the furnace was increased from room temperature to various furnace temperatures (800 °C, 850 °C, 900 °C and 950 °C) at a rate of 30 °C/min and maintained for various growth times (15, 30, 60, 90 and 120 min). Finally, the furnace was cooled down to room temperature. A light gray layer was observed on the alumina substrate. The temperature variation as a function of distance from the center of the furnace was measured which is presented in Fig. 1(b). This temperature profile helps to determine the optimum location of the substrate and growth temperature for the formation of nanowires.

2.2. Characterization

The morphology, structural and elemental distribution of the nanowires were characterized by X-ray diffraction (XRD: Siemens D-5000), field-emission scanning electron microscopy (FESEM: Auriga Zeiss Ultra-60) equipped with an energy dispersive X-ray spectroscopy, and high resolution transmission electron microscopy (HRTEM: FEI Tecnai F-20 microscopy). Selected area electron diffraction (SAED) pattern was also obtained. TEM samples were prepared by sonication of the nanowires extracted from the substrate in deionized water. The nanowire suspension was then drop coated on a carbon-coated copper grid (300 mesh).

2.3. Gas sensing measurements

Zn_2SnO_4 nanowires grown on Au printed interdigitated electrode having a dimension of 5 mm × 5 mm was used as a gas sensor. Gold wire with a diameter of 0.2 mm was connected to Au electrode using Au paste followed by curing at 700 °C for 2 h. The sensor was then placed inside a horizontal tube furnace and sensing measurements were carried out in the presence of various test gases. The sensitivity of the sensor is defined as $(R_a - R_g)/R_g$, where R_a and R_g are the resistances measured in nitrogen and tested gas, respectively. The response and recovery times are determined as the time taken by the sensor to attain 90% of the total resistance change for response and recovery, respectively [36].

3. Results and discussion

3.1. Morphology and structural analysis of Zn_2SnO_4 nanowires

Fig. 2 shows the XRD patterns of Zn_2SnO_4 nanowires obtained for samples prepared by carbon assisted thermal evaporation process at 900 °C for a growth time of 120 min. Ternary compound of face centered cubic spinel Zn_2SnO_4 phase is detected in the XRD patterns which is denoted as ZTO in Fig. 2. These peaks are consistent with the JCPDS card no of 24-1470. Au (111) and alumina peaks are noticed which originate from the gold coated alumina substrate. A small quantity of ZnO phase is also identified. The presence of sharp and strong X-ray diffraction peaks suggests that the Zn_2SnO_4 nanowires have good crystallinity.

We carried out experiments to find the effect of growth times, growth temperature, and substrate position from the center of the furnace on the growth of Zn_2SnO_4 nanowires. Fig. 3 shows the FESEM micrographs of nanostructures grown at different furnace temperatures with various deposition positions, and the growth temperatures of nanostructures at various deposition positions are illustrated in Table 1. At low furnace temperature of 800 °C, no nanowires are observed with different deposition positions (Fig. 3(a)–(d)). The range of growth temperatures between 633 °C and 802 °C are not high enough to produce sufficient Zn and Sn vapour pressure to grow the nanowires (see Table 1) and Au thin film cannot break up into nanosized droplets [37]. Therefore no

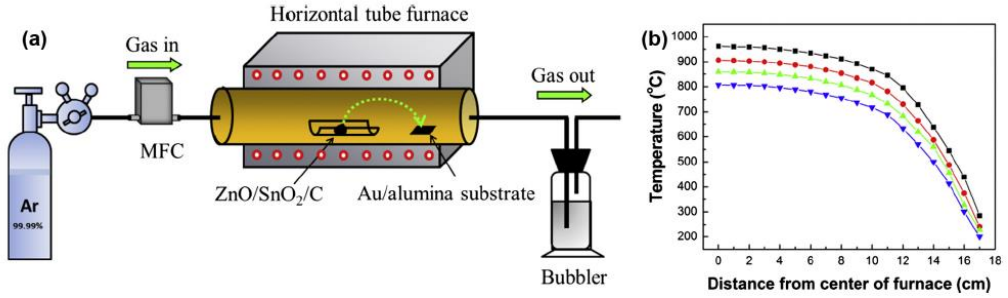

Fig. 1. (a) Experimental setup for the growth of Zn_2SnO_4 nanowires and (b) temperature profile as a function of distance from the center of the furnace at 25 sccm Ar flow.

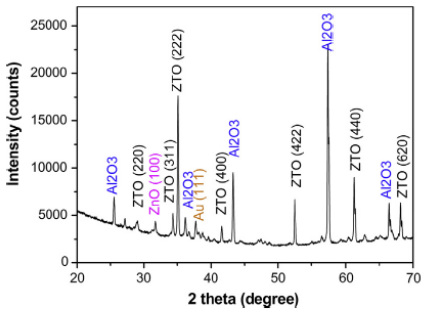

Fig. 2. XRD patterns of Zn_2SnO_4 nanowires.

nanowires are observed. At furnace temperature of 850 °C, nanowires initiate to grow at the substrate position of 6 cm except other places (Fig. 3(e)–(h)). Lengths of nanowires are very short and thicker in diameter. Therefore, the growth temperature of nanowires is found to be around 833 °C (Table 1). At moderate furnace temperature of 900 °C, more heavily populated nanowires are observed at the deposition position of 9 cm in Fig 3(k). The length of nanowires is increased to several tens of micrometres with thinner diameter compared to furnace temperature of 850 °C. The growth temperature of nanowires is observed at 834 °C (Table 1), which is consistent with the furnace temperature of 850 °C at the deposition position of 6 cm. At high furnace temperature of 950 °C, a fewer nanowires are observed anywhere on the substrate (Fig. 3(m)–(p)). This happens because the growth temperatures for various deposition positions are too high for the condensation of metal vapours. Thus no nanowires are observed.

From these results, we can conclude that the optimum growth temperature for nanowire growth is around 834 °C at the deposition position of 9 cm with furnace temperature of 900 °C. Furnace temperatures of 800 °C and 850 °C are not high enough to produce sufficient vapour pressure to grow the nanowires. On the other hand, the furnace temperature of 950 °C is too high for the condensation of the metal vapours.

Fig. 4(a)–(e) exhibits FESEM micrographs for Zn_2SnO_4 nanowires grown on Au/alumina substrate at different growth times. The insets of figures show the single Zn_2SnO_4 nanowire corresponding to the growth time. Growth time was varied from 15 min to 120 min, while the center position temperature of the tube furnace

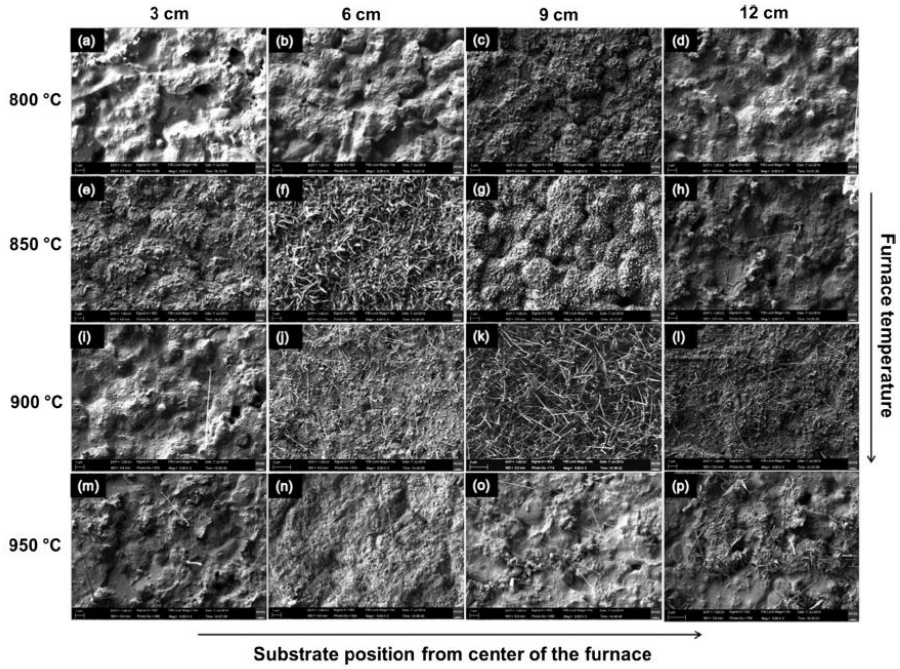

Fig. 3. FESEM images of the nanostructures fabricated at different furnace temperatures with various deposition positions of substrate from the center of the furnace.

Table 1
Growth temperatures of nanostructures obtained at different furnace temperatures and various substrate positions.

Substrate position from center of furnace (cm)	Growth temperatures for different furnace temperatures (°C)			
	800	850	900	950
3	802	854	900	956
6	780	833	880	935
9	737	788	834	893
12	633	684	730	796

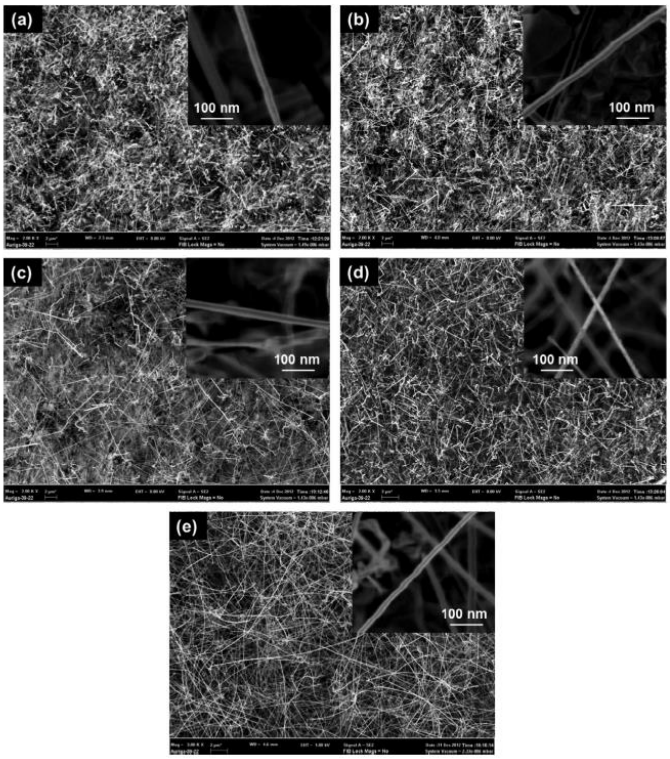

Fig. 4. FESEM micrographs of the nanostructures synthesized at different growth times on Au/alumina substrate at 900 °C: (a) 15 min, (b) 30 min, (c) 60 min, (d), 90 min and (e) 120 min.

was kept at of 900 °C. As can be seen in Fig. 4(a)–(c), Zn_2SnO_4 nanowires grow sparsely on Au/Alumina substrate with 2–6 μm in length. But, Fig. 4(d) and (e) exhibits that the Zn_2SnO_4 nanowires grow homogeneously on the entire Au/Alumina substrate. The length of the nanowires increases from 2 to 50 μm with increasing growth time from 15 min to 120 min. On the other hand, diameter of the nanowire was observed as decreasing tendency with increasing growth time, which were measured around 80 nm, 72 nm, 68 nm, 63 nm and 58 nm for the growth time of 15 min, 30 min, 60 min, 90 min and 120 min, respectively. The decrease in diameter of nanowire may be attributed to the re-evaporation of materials during longer growth time. The smaller nanowire diameter can be explained by the Gibbs–Thomson effect [38]. An increasing reaction time and thereby decreasing supersaturating vapour lead to the diameter of the nanowire become smaller [37]. From this analysis, we can conclude that the concentration and length of Zn_2SnO_4 nanowires increased and diameter of nanowire decreased with increasing growth time.

FESEM image in Fig. 5(a) shows that large quantity of one-dimensional Zn_2SnO_4 nanowires are obtained with an average length of 10 μm and diameter ranging from 20 to 80 nm. It is seen that the nanowire has a distinct tip as clearly shown in the inset of Fig. 5(b). EDAX spectrum of the tip was taken and is shown in Fig. 5(b). It reveals that point scan of the tip confirms the presence of Au, Zn, Sn and O. It is believed that while Zn, Sn and O come from lower layers of Zn_2SnO_4 nanowires, Au is at the tip of the nanowire that acts as a catalyst for the growth of Zn_2SnO_4 nanowire via the vapour–liquid–solid mechanism [39].

Fig. 6 presents a representative scanning-mode TEM (STEM) image of the nanowire and the corresponding Zn, O and Sn elemental maps. As shown in Fig. 6(c)–(e), all elements in the Zn_2SnO_4 nanowire are homogeneously distributed over the entire surface of the nanowire. From the distribution of elements, we can conclude that all nanowires are composed of Zn_2SnO_4. These observations are consistent with Zn_2SnO_4 nanowires obtained via catalyst free growth method by Liang et al. [26].

A representative low magnification TEM image of Zn_2SnO_4 nanowire having an average diameter of 25 nm is depicted in Fig. 7(a). As we can see in Fig. 7(b), the nanowire shows the gold cap at its tip indicating that the growth of nanowire is via the well-known vapour–liquid–solid (VLS) mechanism. The clear lattice fringes in Fig. 7(c) of the HRTEM image show the single crystalline nature of the nanowire with an interplanar spacing of 0.26 nm, which is ascribed to the d-spacing of (311) planes of Zn_2SnO_4 [18,20]. Thus the nanowire growth direction is believed to be [311] [40]. The SAED pattern also demonstrates that the nanowire is a single crystal (Fig. 7(d)).

We propose a growth mechanism for the synthesized Zn_2SnO_4 nanowires from the aforementioned experimental results, which is depicted in Fig. 8. It is believed that the growth is governed by the following chemical reactions.

$$ZnO_{(s)} + SnO_{2(s)} + C_{(s)} \rightarrow Zn_{(v)} + Sn_{(v)} + CO_{(v)}/CO_{2(v)} \quad (1)$$

$$2Zn_{(v)} + Sn_{(v)} + 4CO_{(v)} \rightarrow Zn_2SnO_{4(s)} + 4C_{(s)} \quad (2)$$

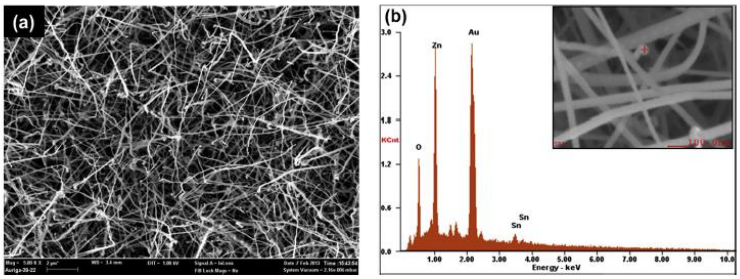

Fig. 5. (a) Typical low magnification FESEM image of Zn_2SnO_4 nanowires and (b) EDAX spectrum of tip of the nanowires.

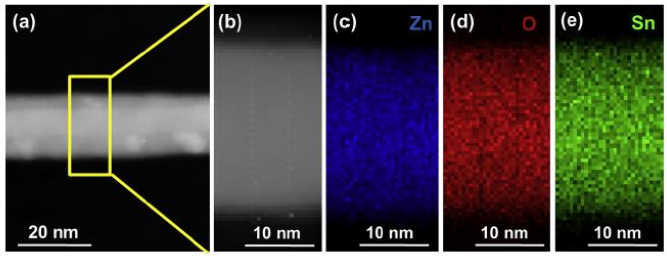

Fig. 6. STEM–EDS analysis of nanowire: (a) STEM image of Zn_2SnO_4 nanowire, (b) enlarged image of the map area in (a), and corresponding mapping elements of Zn (c), O (d), and Sn (e).

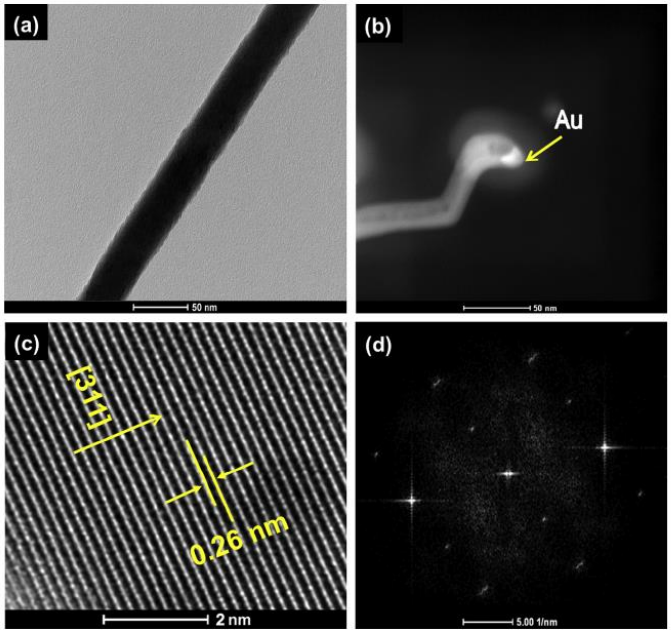

Fig. 7. (a) Low magnification TEM images of a single Zn_2SnO_4 nanowire deposited at 120 min; (b) nanowire with a catalyst at its tip; (c) HRTEM image and corresponding (d) SAED pattern of Zn_2SnO_4 nanowire.

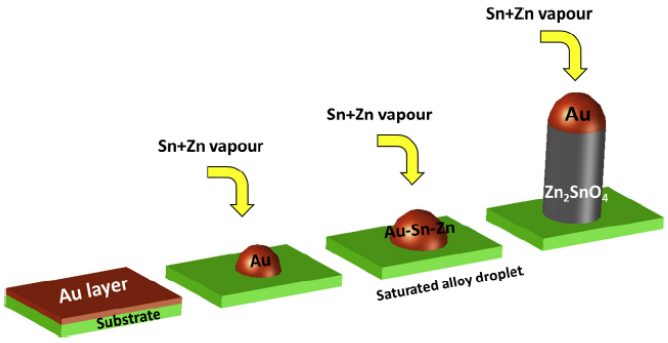

Fig. 8. Schematic representation of Zn_2SnO_4 nanowires grown on Au/alumina substrate.

In this experiment, Zn and Sn are vaporized after reduction by activated carbon in the higher-temperature region (900 °C), which is the center of the furnace temperature. Then the vapours are transported to the substrate which is located downstream at a lower temperature region (~830 °C). The vapour is composed of Zn and Sn that reacts with the gold nanoparticle on the substrate and form Au–Sn–Zn liquid alloy droplet [41]. This alloy further reacts with oxygen and nucleates Zn_2SnO_4 nanowire. Although our experiments were done in purified Ar (99.99%) atmosphere, the oxygen could come from the small amount of oxygen in Ar (10 s of ppm). When more Zn and Sn vapour are dissolved in the liquid droplet, Zn_2SnO_4 would reach the supersaturated state. Subsequently, saturated solid Zn_2SnO_4 precipitates from the droplets in the form of Zn_2SnO_4 nanowires by absorbing more Zn and Sn vapour. So, Zn_2SnO_4 nanowires continue to grow with gold at the tip. On the other hand, carbon soot was observed on the wall of the quartz tube at 18 cm from the center of the furnace. Therefore, the carbon soot has from CO according to reaction (2). It is believed that re-oxidation was performed between Zn–Sn vapours and CO. Therefore, carbon soot was detected on the interior wall of quartz tube.

ZnO nanowires coexist with Zn_2SnO_4 nanowires in our product which is presented in XRD analysis. In this present process, more ZnO is used as compared to SnO_2 (molar ratio between ZnO and SnO_2 is 9:1). It is believed that, ZnO nanowires formed due to different speeds of vaporization of ZnO and SnO_2, and excess ZnO [39]. The control of the evaporation of source mixture is crucial for the synthesis of ternary oxide Zn_2SnO_4 nanowires. Single phase Zn_2SnO_4 ternary oxide nanowires might be acquired under optimum conditions. Jie et al. [39] reported that the ratio between ternary and binary oxide nanowires in the end product is dependent on the growth temperature, substrate position temperature and the ratio of source mixture.

3.2. Gas sensing properties of Zn_2SnO_4 nanowires

The gas sensing tests were conducted for various gases to examine the sensor performance of the Zn_2SnO_4 nanowire. The sensitivity of a gas sensor is usually dependent on an optimum temperature [42]. The sensitivity of the sensor to 20 ppm of ethanol, hydrogen and methane were tested to determine an optimum temperature, which are shown in Fig. 9(a). It can be observed that the sensitivity of the sensor varied with the operating temperature. From the results of ethanol, we can see that the sensitivity increases with temperature up to 500 °C and then decreases. Thus, 500 °C is determined to be the optimum temperature for ethanol detection. Similar trend is also obtained for hydrogen and methane with much less sensitivity compared to ethanol, shown in Fig. 9(a). Very similar values of optimum operating temperature are observed for all gases, though literature indicates varying optimum temperatures for different gases [43]. The variations in the optimum operating temperature for different gases suggest variation in the adsorption and desorption characteristics of the gases. This property is utilized to design selective sensors. However, all sensors are operated over a wide range of temperature (300–550 °C) leading to different thermal energies for the surface reactions [44]. The sensitivity is very low below the operating temperature of 300 °C. It may be attributed to the adsorbed gas molecules not being sufficiently activated to react with the adsorbed oxygen ion species on the surface of the sensing medium [44]. As the temperature is further increased above 300 °C, the activation energy barrier is surmounted allowing gas molecules react with surface adsorbed oxygen leading to the change in resistance and hence enhanced sensitivity [45]. The sensitivity of the sensor is observed to decrease above the temperature of 500 °C. This is a commonly observed phenomenon in resistive sensors since at higher temperatures desorption becomes dominant that leads to the decrease in sensitivity [45,46].

Representative dynamic gas responses of the Zn_2SnO_4 sensor is measured upon exposure to ethanol, hydrogen and methane at 500 °C and the results are shown in Fig. 9(b)–(d). These results imply that the sensor exhibits a strong response for ethanol and very little response for other two gases at 500 °C. One of the key performance indicators for a gas sensor is to have good selectivity. Zn_2SnO_4 nanowire sensor exhibits high selectivity toward ethanol compared to the other two gases. The response increases rapidly with increasing concentration of ethanol from 20 ppm to 400 ppm. This response curve reveals that the sensor could detect ethanol in a wide range. Five cycles were recorded with the concentrations of 20, 50, 100, 250 and 400 ppm. Sensitivities of ethanol corresponding to the above concentrations are 4.9, 21.6, 60.8, 254, and 468, respectively. The sensitivities of hydrogen and methane to 400 ppm are 4.75 and 2.7, respectively, which is around 100 times lower than those for ethanol. The response and recovery times for ethanol are 120 s and 200 s, respectively for the concentration of 20 ppm. Response and recovery times are decreased from 120 s to 100 s and 200 s to 60 s, respectively, with increasing concentration from 20 ppm to 400 ppm. The observed high sensitivity and selectivity of Zn_2SnO_4 nanowires demonstrate that this material is a suitable candidate for monitoring ethanol.

3.3. Gas sensing mechanism of Zn_2SnO_4 nanowires

Gas adsorption and desorption is a common mechanism for gas sensing [47]. Metal oxide based sensor is exposed to air, which results in O_2 adsorption on the surface of the material. Oxygen